

## **PARAMETRIC SPECTRAL ESTIMATION: A PROPER SOLUTION FOR POWER MEASUREMENT IN DIGITAL WIRELESS COMMUNICATION SYSTEMS**

*Leopoldo Angrisan<sup>1</sup>, Aldo Baccigalupi<sup>1</sup>, Antonio Langella<sup>1</sup>, Michele Vadursi<sup>2</sup>*

<sup>1</sup> Dipartimento di Informatica e Sistemistica, Università degli Studi di Napoli Federico II, Italy  
Phone: +390817683170 – Fax: +390812396897 – E-mail: {angrisan; baccigal; langanto}@unina.it

<sup>2</sup> Dipartimento di Ingegneria Elettrica, Università degli Studi di Napoli Federico II, Italy  
Phone/Fax: +390817683866 – E-mail: m vadursi@unina.it

**Abstract:** Poor repeatability and low accuracy often affect power measurements in digital wireless communication systems. A new digital signal processing-based method is proposed, which exploits Marple's solution to parametric spectral estimation in order to achieve the power spectral density (PSD) of the analyzed signal, and then evaluates the quantities of interest by applying straightforward measurement algorithms to the estimated PSD. The performance of the method is assessed through a number of experiments on laboratory signals, and compared to that offered both by an alternative measurement solution, based on a different parametric estimator, and high-performance instruments already available on the market.

**Keywords:** Average power measurement, channel power measurement, occupied bandwidth measurement, digital transmitters testing, digital wireless communication systems.

### **1. INTRODUCTION**

Power measurements are of major concern in any digital wireless communication system. Average power, channel power, occupied bandwidth and adjacent channel power ratio measurements are relevant examples. They are usually carried out by integrating the radiofrequency (RF) signal power spectral density (PSD) over a specified frequency range. In the presence of wideband or spread spectrum signals, their high crest factor (peak to average power ratio) and/or noise-like nature make the aforementioned task quite troublesome to be fulfilled [1],[2].

To overcome the aforementioned problems, the authors have proposed two methods for power measurement in digital wireless communication systems, which are based respectively on non-parametric and parametric PSD estimation [3],[4]. The results of a large number of experiments, on both laboratory and real signals, have shown that both methods allow the mitigation of repeatability and low accuracy problems affecting most instruments currently available on the market. As measurement time required by the method based on parametric spectral estimation is definitely lower than the

other, its use in production and testing stages of digital wireless equipment is encouraged.

Specifically, in [4] the authors chose to develop an algorithm based on Burg's results, which represents a very efficient and popular solution to autoregressive model parameter estimation. It is, in fact, characterized by a one order of magnitude lower complexity with respect to common matrix inversion techniques.

An alternative solution, due to Marple [5], is actually characterized by a computational burden comparable to that peculiar to Burg's solution, and in some cases exhibits improved performance in spectral estimation [6],[7]. Specifically, major improvements consist in less bias in the frequency estimate of spectral components and reduced variance in frequency estimates over an ensemble of spectra. Studies in [6] and [7], however, do not account for signals typical of modern digital wireless communication systems.

The paper investigates whether the adoption of Marple's solution can bring benefits to power measurements involving this type of signals. In particular, a new measurement method is proposed, whose essential structure is the same as in [4], and consists of (i) signal digitization, (ii) parametric PSD estimation, and (iii) application of measurement algorithms to the estimated PSD. The substantial difference dwells in PSD estimation, which is the core of the method; it is, in fact, performed according to Marple's solution.

The performance of the new method is assessed through a number of experimental tests, carried out on WCDMA (Wideband Code Domain Multiple Access) signals peculiar to UMTS (Universal Mobile Telecommunication System), and IEEE 802.11a/b/g WLAN (Wireless Local Area Networks) signals. A thorough comparison between measurement results provided by the new method, and those furnished by the method proposed in [4] is carried out. For the sake of completeness, results provided by both methods are also compared to those delivered by high-performance instruments currently available on the market.

### **2. PROPOSED METHOD**

From an operative point of view, the proposed method can be divided into three stages: (i) RF signal

downconversion and digitization, (ii) power spectral density estimation, and (iii) power measurement.

### 2.1. RF signal downconversion and digitization

As it happens with VSAs (Vector Signal Analyzers) and PSAs (Performance Spectrum Analyzers), the input RF signal is first downconverted to a suitable intermediate frequency, and then digitized by means of a data acquisition system (DAS), the bandwidth of which has to include all significant spectral content of the downconverted signal.

### 2.2. Power spectral density estimation

Some theoretical notes on parametric PSD estimation are first given. Then, the idea behind Marple's solution to parametric spectral estimation is discussed. Finally, the recursive steps of the algorithm implementing such solution for the estimation of the PSD of the signal under test are described.

An autoregressive model of order  $p$ ,  $AR(p)$ , is the most widely used functional form for PSD estimation. A stationary  $AR(p)$  process  $\{Y_t\}$  with zero mean satisfies the equation

$$Y_t = \phi_{1,p} Y_{t-1} + \phi_{2,p} Y_{t-2} + \dots + \phi_{p,p} Y_{t-p} + \varepsilon_t \quad (1)$$

where  $\phi_{1,p}, \phi_{2,p}, \dots, \phi_{p,p}$  are  $p$  fixed coefficients, and  $\{\varepsilon_t\}$  is a white noise process with zero mean and variance  $\sigma_p^2$ .

The PSD for a stationary  $AR(p)$  process is given by

$$S(f) = \frac{\sigma_p^2 T_s}{\left| 1 - \sum_{m=1}^p \phi_{m,p} e^{-j2\pi m f T_s} \right|^2}, \quad |f| \leq f_N, \quad (2)$$

where  $T_s = 1/f_s$  is the time (sampling) interval between consecutive samples in the process, and  $f_N = 1/(2T_s)$  is the Nyquist frequency.

Let  $X_1, X_2, \dots, X_N$  be the acquired samples of the (real-valued) signal under test. A recursive digital signal processing-based approach, based on Marple's solution, is applied to the samples in order to estimate  $\phi_{1,p}, \phi_{2,p}, \dots, \phi_{p,p}$ ,  $\sigma_p^2$ , and, ultimately, the PSD of the signal. The better the arbitrary stationary process  $X_t$  is approximated by an  $AR(p)$  stationary process, the more reasonable is this procedure.

Let  $\bar{\phi}_{1,p}, \bar{\phi}_{2,p}, \dots, \bar{\phi}_{p,p}$  be the current estimates of the coefficients in (1). The forward and backward prediction errors are, respectively, defined as

$$\bar{e}_t(p) \equiv X_{t+p} - \sum_{i=1}^k \bar{\phi}_{i,p} X_{t+p-i}, \quad 1 \leq t \leq N-p \quad (3)$$

and

$$\bar{e}_t(p) \equiv X_t - \sum_{i=1}^k \bar{\phi}_{i,p} X_{t+i}, \quad 1 \leq t \leq N-p \quad (4)$$

As in [4], the coefficients  $\phi_{1,p}, \phi_{2,p}, \dots, \phi_{p,p}$  are estimated by minimizing the prediction error energy, that is the sum of squares of prediction errors, namely

$$SS_p \equiv \sum_{t=1}^{N-p} [\bar{e}_t^2(p) + \bar{e}_t^2(p)] \quad (5)$$

By substituting (3) and (4) in (5), the least square minimum for  $SS_p$  is obtained by nulling the derivatives of  $SS_p$  with respect to the parameters  $\bar{\phi}_{1,p}, \bar{\phi}_{2,p}, \dots, \bar{\phi}_{p,p}$ , that is

$$\frac{\partial SS_p}{\partial \bar{\phi}_{i,p}} = -2 \sum_{j=0}^p \bar{\phi}_{j,p} r_p(i, j) = 0, \quad i = 1, \dots, p \quad (6)$$

with  $\phi_{0,p} = 1$  by definition, where

$$r_p(i, j) = \sum_{k=1}^{N-p} (x_{k+p-j} x_{k+p-i} + x_{k+j} x_{k+i}), \quad 0 \leq i, j \leq p \quad (7)$$

Using the  $p$  equations in (6), along with the expressions (3) and (4), the minimum prediction error energy comes out to be

$$SS_p = - \sum_{j=0}^p \bar{\phi}_{j,p} r_p(0, j) \quad (8)$$

Putting together the expressions (3), (4) and (8), the system

$$\underline{\underline{R}}_p \underline{\underline{\Phi}}_p = \underline{\underline{E}}_p \quad (9)$$

is gained, where

$$\underline{\underline{\Phi}}_p = [1 \quad \bar{\phi}_{1,p} \quad \dots \quad \bar{\phi}_{p,p}]^T \quad (10)$$

$$\underline{\underline{E}}_p = [SS_p \quad 0 \quad \dots \quad 0]^T \quad (11)$$

and

$$\underline{\underline{R}}_p = \begin{bmatrix} r_p(0,0) & \dots & r_p(0,p) \\ \vdots & & \vdots \\ r_p(p,0) & \dots & r_p(p,p) \end{bmatrix} \quad (12)$$

In [9] and [10], all terms in the matrix (12) are directly computed, and then the system (9) is solved through matrix inversion. This requires a number of operations proportional to  $p^3$ , which is about one order of magnitude greater than the solution adopted in [4]. Further details can be found in [8].

As suggested by Marple in [5], the actual structure of the matrix (12) requires a number of operations proportional to  $p^2$ . This result motivates the interest in investigating a possible use of Marple's solution to parametric spectral estimation. Specifically, the matrix (12) can be written as

$$\underline{\underline{R}}_p = \underline{\underline{T}}_p^T \underline{\underline{T}}_p + \underline{\underline{T}}_p^{(r)T} \underline{\underline{T}}_p^{(r)} \quad (13)$$

where the matrix  $\underline{\underline{T}}_p$  is a  $(N-p) \times (p+1)$  Toeplitz matrix containing samples of the signal under test:

$$\underline{\underline{T}}_p = \begin{bmatrix} x_{p+1} & x_p & \dots & x_1 \\ x_{p+2} & x_{p+1} & \dots & x_2 \\ \vdots & \vdots & & \vdots \\ x_N & x_{N-1} & \dots & x_{N-p} \end{bmatrix} \quad (14)$$

and  $\underline{\underline{T}}_p^{(r)}$  is the reversed matrix, that is

$$\underline{T}_p^{(r)} = \begin{bmatrix} x_1 & x_2 & \cdots & x_{p+1} \\ x_2 & x_3 & \cdots & x_{p+2} \\ \vdots & \vdots & & \vdots \\ x_{N-p} & x_{N-p+1} & \cdots & x_N \end{bmatrix}. \quad (15)$$

Structure (13) can be exploited by introducing two additional error energy terms

$$SS_p' \equiv \sum_{t=1}^{N-p-1} [\bar{e}_{t+1}^2(p) + \bar{e}_t^2(p)] \quad (16)$$

and

$$SS_p'' \equiv \sum_{t=1}^{N-p-1} [\bar{e}_t^2(p) + \bar{e}_{t+1}^2(p)] \quad (17)$$

and minimizing them according to the same procedure adopted for (6). This way, the expressions

$$\underline{R}_p' \underline{\Phi}_p' = \underline{E}_p' \quad (18)$$

$$\underline{R}_p'' \underline{\Phi}_p'' = \underline{E}_p'' \quad (19)$$

are obtained, where  $\underline{\Phi}_p'$  and  $\underline{\Phi}_p''$  are defined, respectively, as

$$\underline{\Phi}_p' = [1 \quad \bar{\phi}'_{1,p} \quad \cdots \quad \bar{\phi}'_{p,p}]^T \quad (20)$$

$$\underline{\Phi}_p'' = [1 \quad \bar{\phi}''_{1,p} \quad \cdots \quad \bar{\phi}''_{p,p}]^T \quad (21)$$

and  $\underline{E}_p'$  and  $\underline{E}_p''$  are given, respectively, by

$$\underline{E}_p' = [SS_p' \quad 0 \quad \cdots \quad 0]^T \quad (22)$$

$$\underline{E}_p'' = [SS_p'' \quad 0 \quad \cdots \quad 0]^T \quad (23)$$

whereas the elements of  $\underline{R}_p'$  and  $\underline{R}_p''$  are expressed, respectively, as

$$r_p'(i, j) = \sum_{k=1}^{N-p-1} (x_{k+p+1-j} x_{k+p+1-i} + x_{k+j} x_{k+i}) \quad (24)$$

$$r_p''(i, j) = \sum_{k=1}^{N-p-1} (x_{k+p-j} x_{k+p-i} + x_{k+1+j} x_{k+1+i}) \quad (25)$$

for  $0 \leq i, j \leq p$ . Some manipulations show that the recursive relationship

$$\bar{\phi}_{i,k} = \bar{\phi}'_{i,k-1} - \bar{\phi}_{k,k} \bar{\phi}'_{k-i,k-1}, \quad 1 \leq i \leq k-1, \quad (26)$$

holds for the AR parameters, and that

$$\bar{\phi}_{k,k} = -\frac{[r_k(k, 0) \quad \cdots \quad r_k(k, k-1)] \underline{\Phi}_{k-1}'}{SS_{k-1}'}. \quad (27)$$

Further details can be found in [5].

The recursive procedure, which exploits Marple's solution is characterized by the following fundamental steps.

1. The vector  $\underline{\Phi}_{k-1}'$  and the term  $SS_{k-1}'$  are estimated according to the results found in [5].
2. The  $k$  terms  $r_k(k, j)$ ,  $j=0, \dots, k-1$ , are computed from the

samples of the signal under test.

3. Expression (27) is evaluated to achieve an estimate of  $\bar{\phi}_{k,k}$ .
4. If  $\bar{\phi}_{k,k} < \frac{2}{\sqrt{N}}$ , the process is halted, and the order  $p$  is put equal to  $k-1$ ; otherwise, the step 5 is taken.
5. Estimates of the AR coefficients are updated by evaluating  $\bar{\phi}_{1,k}, \bar{\phi}_{2,k}, \dots, \bar{\phi}_{k-1,k}$  from the expression (26).

Once the recursive procedure is halted,  $\sigma_p^2$  is evaluated according to [5]

$$\sigma_p^2 = SS_{p-1}' (1 - \phi_{p,p}^2) \quad (28)$$

and the PSD is gained by substituting the estimates of the AR parameters  $\bar{\phi}_{1,p}, \bar{\phi}_{2,p}, \dots, \bar{\phi}_{p,p}$  and  $\sigma_p^2$  into the expression (2).

The criterion used to select the order of the AR process is one of the alternatives enlisted in [8]. The rationale for such choice is that for a Gaussian AR( $p$ ) process, the  $\bar{\phi}_{k,k}$  terms for  $k > p$  are, approximately, independently distributed with zero mean and a variance equal about to  $1/N$  [12].

### 2.3. Power measurement

Once the PSD of the analyzed signal has been estimated, power measurements can be carried out by means of very straightforward algorithms. In particular, average power, channel power and occupied bandwidth measurements are taken into account.

Average power is evaluated by integrating the estimated PSD over the whole frequency span analyzed.

With regard to channel power, the frequency interval, centered at the tune frequency of the monitored channel and whose extent is as wide as the channel spacing of the specific system, is first established; then, the desired power is obtained by integrating the PSD over the aforementioned frequency interval.

Concerning occupied bandwidth, it is defined as the frequency interval, centered at the tune frequency of the monitored channel, over which the integral of the estimated PSD equals 99% of the average power. Occupied bandwidth is calculated as the difference  $f_2 - f_1$  between the two frequency values,  $f_2$  and  $f_1$ , which make each of the two frequency intervals  $[f_2, f_s/2]$  and  $[0, f_1]$  contain 0.5% of the average power.

## 3. EXPERIMENTS

An extended experimental activity has been conducted to assess the performance of the method. WCDMA and IEEE 802.11a/b/g WLAN signals have been considered.

### 3.1. Measurement station and procedure

A proper measurement station has been set up, which is depicted in Figure 1. The station has consisted of 1) a processing and control unit, namely a personal computer (PC), 2) a data acquisition system (DAS), *Agilent Technologies Infiniium DSO81004A<sup>TM</sup>* (8-bit resolution,

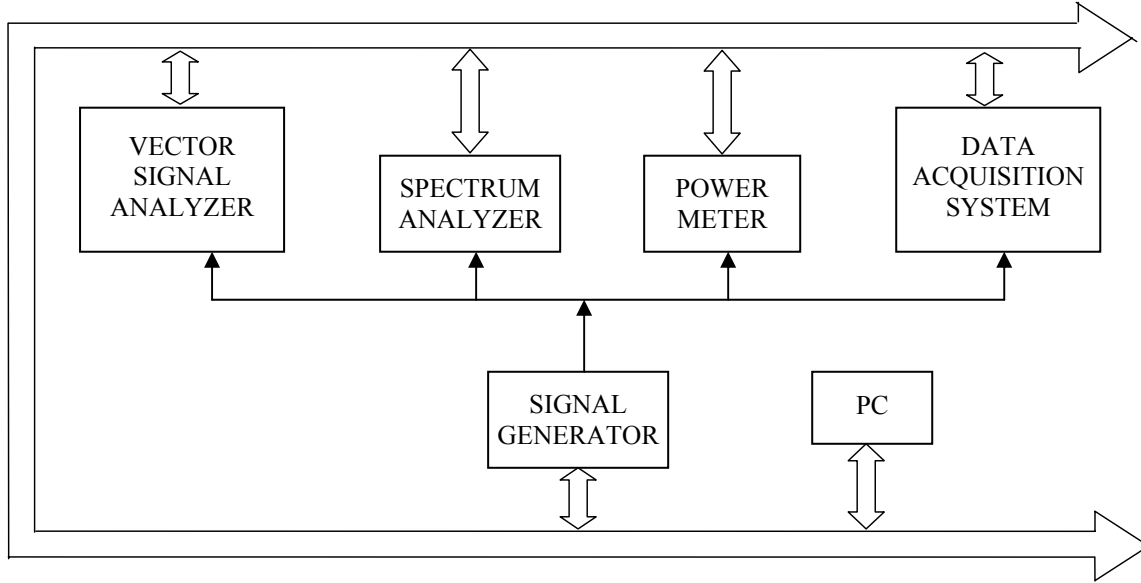


Figure 1. Measurement station.

10 GHz bandwidth, 40 GS/s maximum sample rate), 3) a spectrum analyzer, *Anritsu MS2687B<sup>TM</sup>* (9 kHz-30 GHz input frequency range, up to 20 MHz resolution bandwidth), 4) a vector signal analyzer (VSA), *Agilent Technologies E4406<sup>TM</sup>* (7 MHz-4 GHz input frequency range), 5) an RF power meter, *Agilent Technologies E4416A<sup>TM</sup>* (100 kHz-6.0 GHz input frequency range) and 6) a digital RF signal generator, *Agilent Technologies E4438C<sup>TM</sup>* (250 kHz-6.0 GHz output frequency range, I/Q analog inputs) with arbitrary waveform generation capability (14-bit vertical resolution, 8 MS memory depth, 100 MHz sample clock). The digital RF signal generator has been commanded to generate RF digitally modulated signals compliant either with IEEE 802.11 a/b/g standards or WCDMA specifications. In particular, while the digital RF signal generator has the capability of directly synthesizing WCDMA signals, samples of IEEE 802.11 test signals have to be synthesized through a specific signal generation software, *Agilent Technologies E4438C-417 Signal Studio*

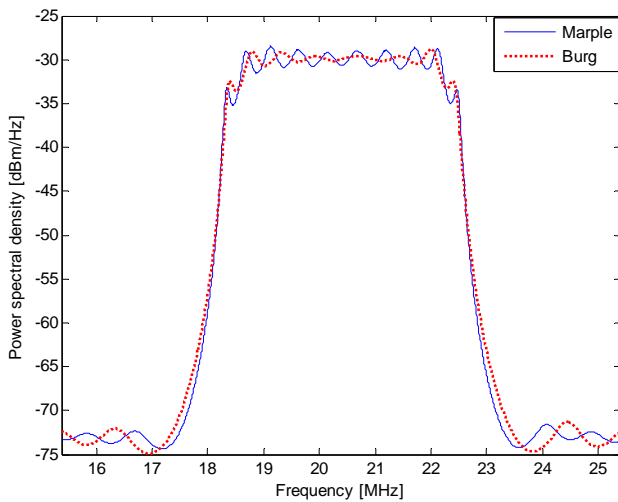


Figure 2. Comparison of the PSD of the WCDMA downlink test signal estimated through the proposed parametric method (solid line) to that estimated through the solution presented in [4] (dotted line).

for 802.11 WLAN<sup>TM</sup>, and downloaded into the memory of the digital RF signal generator. All the instruments have been interconnected by means of an IEEE-488 standard interface bus.

The RF signal provided by the generator has been the input of the DAS, which has digitized it according to a specified sample rate, exploiting *ad hoc* band-pass sampling techniques [13]. The digitized samples have then been transferred to the PC, on which the digital signal processing algorithm implementing both the second and third stage of the proposed method has been available. On the same PC, the measurement algorithm related to the method described in [4] has also been operative. The same signal has been the input of the other instruments included in the measurement

Table 1. Average power measurement results on a downlink WCDMA test signal.

	$\mu$ [dBm]	$\sigma$ [dBm]
<i>Marple</i>	-10.30	-41.06
<i>Burg</i>	-10.30	-41.55
<i>RF power meter</i>	-10.16	-35.82

Table 2. Channel power measurement results on a downlink WCDMA test signal.

	$\mu$ [dBm]	$\sigma$ [dBm]
<i>Marple</i>	-10.50	-40.14
<i>Burg</i>	-10.51	-39.92
<i>VSA</i>	-10.50	-35.90
<i>Spectrum analyzer Anritsu</i>	-10.40	-33.02

Table 3. Occupied bandwidth measurement results on a downlink WCDMA test signal.

	$\mu$ [MHz]	$\sigma$ [MHz]
<i>Marple</i>	4.288	0.001
<i>Burg</i>	4.289	0.001
<i>Spectrum analyzer Anritsu</i>	4.165	0.003

station. In particular, the power meter has been utilized for average power measurements, whereas the spectrum analyzers have been exploited to evaluate channel power and occupied bandwidth.

### 3.2. Results obtained on WCDMA signals

Experimental tests have been conducted on different types of uplink and downlink WCDMA signals. Signals have been sampled at a rate equal to 100 MS/s [13]. Each measurement has been performed on a record of 16384 samples. For the sake of brevity, only the results related to a downlink WCDMA test signal are discussed in the following. When performing such tests, the carrier frequency has been set equal to 1.7214 GHz and the nominal output power has been equal to -10dBm.

Table 1, Table 2 and Table 3 summarize the results of average power, channel power and occupied bandwidth measurements, respectively. Results are expressed in terms of average value  $\mu$  (over 50 measurements), and experimental standard deviation,  $\sigma$ . Figure 2 compares the PSD of the WCDMA downlink signal estimated through the proposed parametric method (solid line) to that estimated through the solution presented in [4] (dotted line). The PSD estimated through the proposed method exhibits some oscillations that are not present in the other case. At a glance, however, concurrent values of both power level and bandwidth are achieved in the two cases. This is actually confirmed by the results reported in the tables.

### 3.3. Results obtained on IEEE 802.11 signals

Table 4, Table 5 and Table 6 enlist the results achieved through the proposed method, the alternative method presented in [4], and other specialized instruments included in the measurement station. They are related to average power, channel power and occupied bandwidth measurements, respectively. The VSA has not been operative because its frequency span is limited to 10 MHz, which is less than the frequency bandwidth of 802.11 signals.

For the sake of brevity, only some of the results are enlisted.

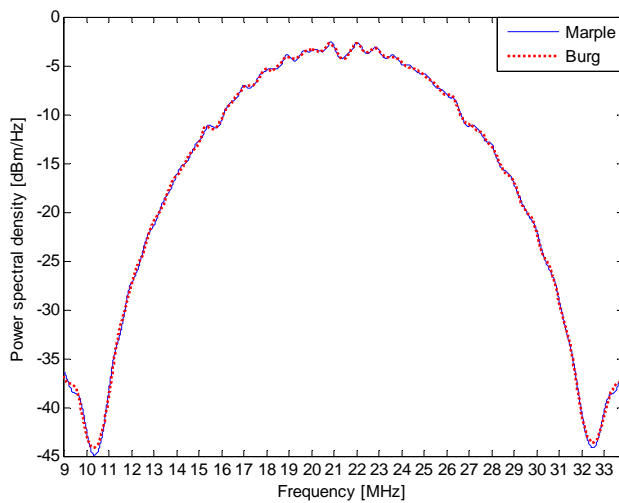


Figure 3. Comparison of the PSD of the IEEE 802.11b test signal estimated through the proposed parametric method (solid line) to that estimated through the solution presented in [4] (dotted line).

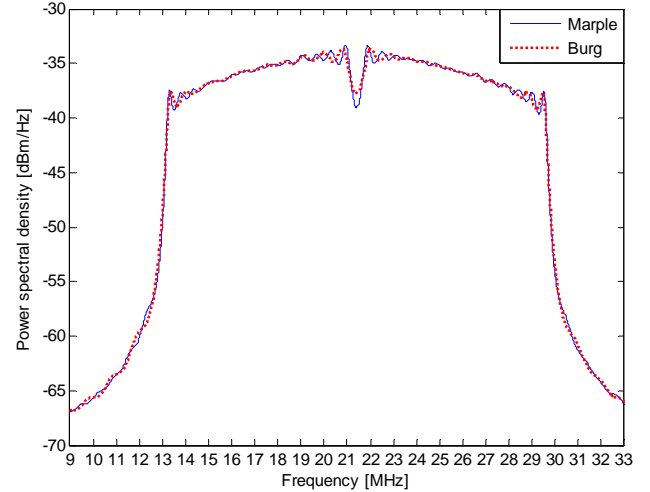


Figure 4. Comparison of the PSD of the IEEE 802.11a test signal estimated through the proposed parametric method (solid line) to that estimated through the solution presented in [4] (dotted line).

They refer to signals whose carrier frequency has been set equal to 1.7214 GHz and nominal output power has been equal to -10dBm. Signals have been sampled at a rate equal to 100 MS/s. Each measurement has been performed on a record of 16384 samples. Experimental outcomes are very similar to those experienced with WCDMA signals.

Table 4. Average power measurement results on IEEE 802.11 signals.

	802.11a		802.11b		802.11g	
	$\mu$ [dBm]	$\sigma$ [dBm]	$\mu$ [dBm]	$\sigma$ [dBm]	$\mu$ [dBm]	$\sigma$ [dBm]
<i>Marple</i>	-10.10	-31.76	-10.60	-33.45	-10.60	-34.08
<i>Burg</i>	-10.10	-31.79	-10.61	-33.50	-10.60	-34.10
<i>RF power meter</i>	-10.25	-35.30	-10.19	-33.78	-10.17	-35.50

Table 5. Channel power measurement results on IEEE 802.11 signals.

	802.11a		802.11b		802.11g	
	$\mu$ [dBm]	$\sigma$ [dBm]	$\mu$ [dBm]	$\sigma$ [dBm]	$\mu$ [dBm]	$\sigma$ [dBm]
<i>Marple</i>	-10.11	-31.76	-10.61	-33.47	-10.61	-34.10
<i>Burg</i>	-10.10	-31.78	-10.60	-33.49	-10.60	-34.15
<i>Spectrum analyzer Anritsu</i>	-10.09	-34.13	-10.84	-36.20	-10.84	-32.90

Table 6. Occupied bandwidth measurement results on IEEE 802.11 signals.

	802.11a		802.11b		802.11g	
	$\mu$ [MHz]	$\sigma$ [MHz]	$\mu$ [MHz]	$\sigma$ [MHz]	$\mu$ [MHz]	$\sigma$ [MHz]
<i>Marple</i>	16.49	0.01	14.97	0.01	14.96	0.01
<i>Burg</i>	16.38	0.01	14.96	0.01	14.98	0.01
<i>Spectrum analyzer Anritsu</i>	16.30	0.01	14.83	0.01	14.84	0.02

### 3.4. Comments

From the analysis of the experimental results the following considerations can be drawn.

- Power and occupied bandwidth measurements exploiting parametric spectral estimation grant very good repeatability. In fact, repeatability is generally comparable or better than that characterizing results provided by instruments.
- The two methods based on parametric spectral estimation provide comparable results both in terms of repeatability (they exhibit comparable experimental standard deviation), and concurrence. None of the two methods can be considered preferable in terms of reduced repeatability.
- Measurement time required by the two methods is comparable.

Besides granting concurrence of power measurement results, the two methods furnish very similar outcomes even in the PSD estimation. To this concern, Figure 3 shows the PSD of an 802.11b signal estimated through the two parametric methods. In particular, the solid line is the PSD estimated through the proposed method, whereas the dotted line refers to the method presented in [4]. Similarly, Figure 4 compares the PSD of an 802.11a signal estimated through the two methods. In both cases the two plots given by the two parametric methods are practically coincident. Estimated PSD is not different from that provided by the spectrum analyzer, which is depicted in Figure 5.

To sum up, the two parametric spectral estimation methods have provided concurrent results in all the experiments, and have been characterized by comparable experimental standard deviations. Except for the PSD shown in Figure 2, they have also provided very similar PSD estimates. The benefits which could be expected as a consequence of the adoption of Marple's solution as the core of the new measurement method have not practically been observed. This can be ascribed to two reasonable facts: (i) studies in [6] and [7] were not conducted on wideband signals, and (ii) power measurements in digital wireless communication systems are basically carried out by integrating the PSD over a specified frequency range. Possible advantages that could be obtained in the PSD estimate vanish when the PSD is integrated to give the measurement result.

### 4. CONCLUSION

A new method for power measurements in digital wireless communication systems has been presented. The core of the method is the estimation of the PSD of the signal under test through a parametric approach based on Marple's solution. A large number of experiments carried out on actual signals have shown that the proposed method grants as good repeatability as that offered by an alternative method, based on a different parametric spectral estimation solution [4]. Measurement time is comparable, as well.

Although the proposed method does not produce significant enhancements with respect to [4], the experimental campaign has confirmed the good results already achieved in [4]. Specifically, power measurements

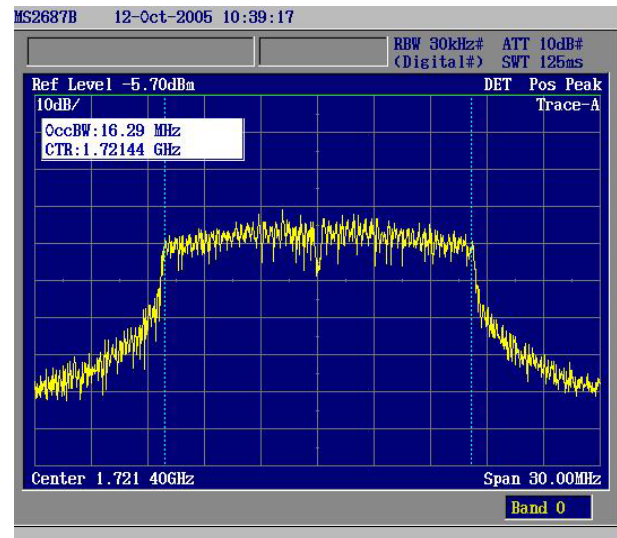


**Figure 5. PSD of IEEE 802.11a signal provided by Anritsu spectrum analyzer (occupied bandwidth measurement result is also displayed).**

that exploit parametric spectral estimation operate with success in digital wireless communication systems; they allow major limitations of specialized instruments currently available on the market to be overcome.

### REFERENCES

- [1] L. Angrisani, M. D'Apuzzo, M. D'Arco, "New digital signal-processing approach for transmitter measurements in third generation Telecommunications systems," *IEEE Trans. on Instrum. and Meas.*, vol. 53, No.3, pp. 622-629, June 2004.
- [2] "Comparing power measurements on digitally modulated signals," Product Note Agilent 8560E/8590E Spectrum Analyzers, Agilent Technologies Literature no. 5968-2602E, 2000.
- [3] L. Angrisani, M. D'Apuzzo, M. D'Arco, "A New Method for Power Measurements in Digital Wireless Communication Systems," *IEEE Trans. on Instrum. and Measur.*, vol.52, No.4, August 2003, pp.1097-1106.
- [4] L. Angrisani, M. D'Apuzzo, M. Vadursi, "Power Measurement in Digital Wireless Communication Systems through Parametric Spectral Estimation," *IEEE Trans. on Instrum. and Meas.*, vol.55, No.4, August 2006, *in press*.
- [5] L. Marple, "A New Autoregressive Spectrum Analysis Algorithm," *IEEE Trans. on Acoustic, Speech, and Signal Processing*, vol.28, No.4, Aug. 1980, pp.441-454.
- [6] L. Marple, *Digital Spectral Analysis with Applications*, Englewood Cliffs, New Jersey, Prentice-Hall, 1987.
- [7] S. M. Kay, *Modern Spectral Estimation: Theory and Application*, Englewood Cliffs, New Jersey, Prentice-Hall, 1988.
- [8] D. Percival, A. Walden, "Spectral Analysis for Physical Applications. Multitaper and Conventional Multivariate Techniques," Cambridge University Press, 1998.
- [9] T. J. Ulrych, R. W. Clayton, "Time series modeling and maximum entropy," *Phys. Earth and Plan. Int.*, vol.12, Aug. 1976, pp.188-200.
- [10] A. H. Nuttal, "Spectral analysis of a univariate process with bad data points, via maximum entropy and linear predictive techniques," Naval Underwater Systems Center, New London, CT, Tech. Rep. 5303, Mar. 26, 1976.
- [11] M. Morf, B. Dickinson, T. Kailath, A. Vieira, "Efficient solutions of covariance equations for linear prediction," *IEEE Trans. on Acoust., Speech, Signal Processing*, vol.ASSP-25, pp.429-433, Oct.1977.
- [12] S. M. Kay, J. Makhoul, "On the Statistics of the Estimated Reflection Coefficients of an Autoregressive Process," *IEEE Trans. on Acoustic, Speech, and Signal Processing*, vol.31, No.6, 1983, pp.1447-1455.
- [13] L. Angrisani, M. Vadursi, "Automatic Selection of Optimal Sample Rate for Band-Pass Signals," *Proc. of IEEE Instr. and Meas. Tech. Conf. IMTC 2006*, Sorrento, Italy, 24-27 April 2006, pp.1430-1435.